



## Recrystallization and micronization of sulfathiazole by applying the supercritical antisolvent technology

Yen-Ming Chen, Muoi Tang, Yan-Ping Chen\*

Department of Chemical Engineering, National Taiwan University, Taipei 106, Taiwan, ROC

### ARTICLE INFO

#### Article history:

Received 12 April 2010

Received in revised form 16 August 2010

Accepted 31 August 2010

#### Keywords:

Supercritical antisolvent

Recrystallization

Micronization

Sulfathiazole

Polymorph

### ABSTRACT

Recrystallization and micronization for an antibacterial active pharmaceutical ingredient (API), sulfathiazole, was investigated in this study using the supercritical antisolvent (SAS) technology. The effects for the type of solvent, temperature and pressure on particle formation were investigated using the SEM, DSC and XRD analyses. It was observed that various solvents resulted in different polymorphisms. The original sulfathiazole had the crystal form III. It was recrystallized and micronized into form I when acetone was used as the solvent in the semicontinuous SAS process. The polymorph changed to form IV when ethanol was employed as the solvent. The mean particle size of sulfathiazole was reduced from its original  $43.0 \pm 15.5 \mu\text{m}$  to  $2.1 \pm 0.8 \mu\text{m}$  at the optimal operating condition. The optimally micronized sulfathiazole exhibited a much narrower particle size distribution. It also presented an enhanced dissolution rate by 3.2 times to the original API in a simulated intestinal fluid.

© 2010 Elsevier B.V. All rights reserved.

### 1. Introduction

Supercritical fluid processes are recognized as advanced technologies for the production of micro- or nano-composite particles [1] with the advantage of reduction of organic solvents in traditional methods. Many discussions on the application of supercritical fluid technologies have been presented in literature [2–8] for particle formation of value added products like pharmaceutical compounds. The most commonly used supercritical fluid is carbon dioxide owing to its low critical properties and the safety consideration. Recrystallized and micronized active pharmaceutical ingredients (APIs) were obtained by employing supercritical CO<sub>2</sub> either as solvent or antisolvent. Much smaller APIs with narrower particle size distribution and preferred morphology are desired in pharmaceutical manufacturing. New polymorphisms can also be obtained with enhanced bioavailability and improved dissolution rate. The required dosage and possible side effect can also be reduced from supercritical CO<sub>2</sub> treated API.

Among various supercritical fluid particle formation techniques, supercritical antisolvent (SAS) process has widely been applied for APIs with limited solubility in supercritical CO<sub>2</sub>. The API was

firstly dissolved in an appropriate solvent, and it was recrystallized in a short period of time due to the supersaturation of API upon introducing high pressure antisolvent CO<sub>2</sub>. We have successfully micronized sulfamethoxazole using SAS process in our previous study [9]. The recrystallization and micronization for another API of sulfathiazole were investigated in this study using the semicontinuous SAS process. Sulfathiazole is an effective antibacterial drug for the treatment of gonorrhoea, bacterial pneumonia, and other bacterial infections. Its solubility in supercritical CO<sub>2</sub> has been measured by Kordikowski et al. [10]. The recrystallization of sulfathiazole has been presented by Yeo et al. [11] using batch SAS process where the resulted mean particle size was about 15  $\mu\text{m}$ . Caputo and Reverchon [12] have presented the micronization of sulfathiazole using urea as the crystal habit modifier to obtain spherical particles with submicron mean size. The optimal operating parameters for semicontinuous SAS process of sulfathiazole were experimentally determined in this work in order to obtain particles with mean size of 1–5  $\mu\text{m}$ . The particle size in this range is feasible for inhalation drug delivery. One motivation of this study was to investigate the solvent effect on the production of different polymorphs of sulfathiazole from the SAS process. Furthermore, the dissolution rates for the original and SAS treated sulfathiazole particles were also newly measured in a simulated intestinal fluid to justify its further application in pharmaceutical industry. Two mathematical models were newly employed in this study to correlate the experimental dissolution rate data of SAS processed sulfathiazole. Quantitative results for the enhancement of dissolution rate and the novelty in dissolution behavior after the SAS process are also examined.

\* Corresponding author at: Department of Chemical Engineering, National Taiwan University, No. 1, Roosevelt Road, Section 4, Taipei 106, Taiwan, ROC.  
Tel.: +886 2 2366 1661; fax: +886 2 2362 3040.

E-mail address: [ypchen@ntu.edu.tw](mailto:ypchen@ntu.edu.tw) (Y.-P. Chen).

### Nomenclature

$a, b$	adjustable parameters in Weibull model
$D$	diffusion coefficient
$f_1$	difference factor
$f_2$	similarity factor
$h_d$	thickness of the diffusion boundary layer
$k_1$	first order release constant in the Noyes–Whitney model
$k_w$	dissolution rate coefficient in the Weibull model
$M$	molecular weight
$m$	accumulated dissolved fraction
$n$	number of experimental data points
$R_i$	percentage of dissolved original sulfathiazole
$S_a$	contacted surface area
$T_i$	percentage of dissolved SAS treated sulfathiazole
$T_m$	melting temperature
$t$	time
$V$	volume

## 2. Experimental

### 2.1. Chemicals

Carbon dioxide (CO<sub>2</sub>) was purchased from San-Fu Chemical Company, Taiwan, with a minimum purity of 99.8 mass%. Sulfathiazole (C<sub>9</sub>H<sub>9</sub>N<sub>3</sub>O<sub>2</sub>S<sub>2</sub>) was purchased from Sigma–Aldrich Company with a minimum purity of 99%. Acetone (C<sub>3</sub>H<sub>6</sub>O) and ethanol (C<sub>2</sub>H<sub>6</sub>O) were purchased from Merck Company with a minimum purity of 99%. Monobasic potassium phosphate (KH<sub>2</sub>PO<sub>4</sub>) and sodium hydroxide (NaOH) were purchased from Sigma–Aldrich and Merck Companies, respectively, with a minimum purity of 99% for preparing the dissolution medium in the measurement of dissolution rate. The structure of sulfathiazole and the melting temperatures of its five polymorphic forms [13,14] are listed in Table 1.

### 2.2. Experimental apparatus and procedures

#### 2.2.1. Particle micronization using semicontinuous SAS process

A semicontinuous SAS process was employed in this study to micronize sulfathiazole. The experimental system was shown in Fig. 1. High pressure CO<sub>2</sub> was charged by a HPLC pump (SSI, Prep 100) into the precipitator from the outside of a coaxial nozzle until the pressure and flow rate attained the steady values. The CO<sub>2</sub> flow rate was measured by a rotameter and was adjusted to 1 L/min (converted at the ambient condition) using the micrometering valve at the exit of the precipitator. Pressure and temperature in precipitator were controlled by a back pressure regulator (Tescom) and heating jacket, respectively. The estimated accuracies for measured temperature and pressure were ±0.1 K and ±0.03 MPa, respectively. The solution of sulfathiazole in solvent was then introduced by another HPLC pump (SSI, Series II) through a capillary nozzle (15 cm long and internal diameter of 100 μm or 200 μm) into the precipitator from the inside of coaxial nozzle. The

volume of the precipitator was 75 mL. The solution of sulfathiazole contacted with supercritical CO<sub>2</sub> in the precipitator. This caused a rapid volume expansion, a decrease in liquid phase density, and resulted in the supersaturation and recrystallization of sulfathiazole in a short time period. The micronized sulfathiazole particles from this fast process were collected on the frit with pore sizes of 0.5 μm at the bottom of the precipitator. After the SAS process, CO<sub>2</sub> was kept flowing through the precipitator as the drying process for 1 h to remove the residual solvent inside the precipitator. The recoveries for the micronized sulfathiazole under all operation conditions were about 60–80%.

#### 2.2.2. Characterization of products

The morphologies of the original and SAS treated sulfathiazole were examined using the scanning electron microscope (SEM, JEOL, JSM-5600). The particle size and size distribution can be measured by either counting the particles from SEM images using software, or by using dynamic laser scattering [15]. For the purpose of screening the optimal process condition, this study determined the particle sizes and their distributions using the image analysis software ImageJ [16]. At least 500 particles were counted from SEM images to determine the mean particle size and particle size distribution. For particles with irregular shapes, we measured the longest distance of opposite angles. The volume percentage particle size distributions before and after the best operation condition were also compared using dynamic laser scattering (Coulter LS 230). The crystal structures of particles were studied using the differential scanning calorimetry (Perkin Elmer, Jade DSC) with a heating rate of 5 K/min, and the X-ray diffractometer (PANalytical, X'Pert) where data were collected with 2θ from 5° to 40° with a scanning rate of 3°/min.

#### 2.2.3. Dissolution rate test

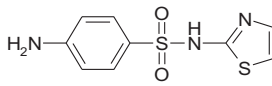
Dissolution rates of the original and micronized sulfathiazole particles were experimentally measured according to the criteria of the USP [17]. The experiments were conducted in a simulated intestinal fluid of 900 mL with pH value of 6.8. This dissolution medium was prepared from an aqueous solution of monobasic potassium phosphate and sodium hydroxide. The temperature of this dissolution medium was kept at 310 K, and the speed of the agitator was at 50 rpm. Accurately weighed samples were added into the suspended basket in the dissolution medium. A small amount of the solution was withdrawn at selected time intervals and filtered through syringe filter with pore size of 0.45 μm. The dissolved amount of sulfathiazole in the dissolution medium was detected using an UV/vis spectrophotometer (Shimadzu, UV-1800) by measuring the absorbance at a wavelength of 280 nm.

## 3. Results and discussion

### 3.1. Micronization of sulfathiazole using SAS process

Two solvents of acetone and ethanol were used in this study. The solubilities of sulfathiazole at room temperature were determined by gravimetric method as 14.93 mg/mL in acetone, and 4.23 mg/mL in ethanol. The effects of six process parameters on

**Table 1**  
Characteristic properties of sulfathiazole.

Compound	CAS	Formula	$M$ (kg/mole)	$T_m$ (K) [13,14]	Structure
Sulfathiazole	72-14-0	C <sub>9</sub> H <sub>9</sub> N <sub>3</sub> O <sub>2</sub> S <sub>2</sub>	0.2553	474–475 (form I) 469–470 (form II) 446–448 (form III) 423–443 (form IV) 448 (form V)	

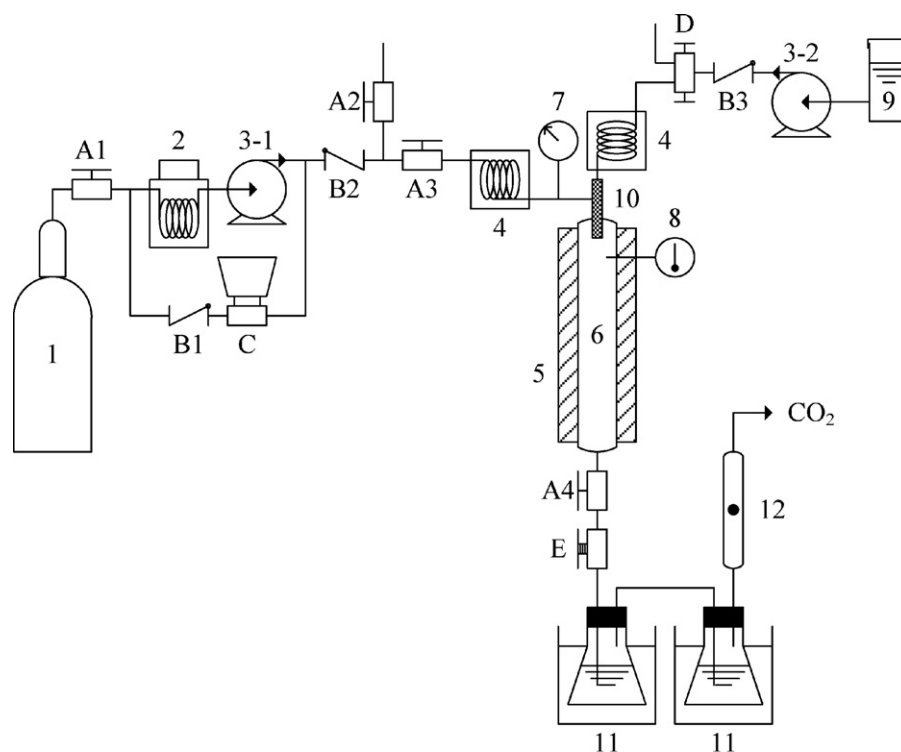


**Fig. 1.** Semicontinuous supercritical antisolvent (SAS) process apparatus. *Valve description:* (A) two-way needle valve; (B) check valve; (C) back pressure regulator; (D) three-way needle valve; (E) micrometering valve. *Element description:* (1) CO<sub>2</sub> cylinder; (2) cooler; (3) HPLC pump; (4) pre-heater; (5) heating jacket; (6) precipitator; (7) pressure transducer; (8) thermometer; (9) solution reservoir; (10) coaxial nozzle; (11) solvent cold trap; (12) rotameter.

the particle sizes, morphologies and polymorphs of sulfathiazole were investigated in this study. These six parameters were the type of solvent (*S*), solution concentration (*C*), temperature (*T*), pressure (*P*), solution flow rate (*F*) and nozzle diameter (*D<sub>n</sub>*). All experimental results are listed in Table 2 and discussed as follows.

### 3.1.1. The effect of solvent and solution concentration

In the investigations of solvent and solution concentration effects, the experimental temperature, pressure, solution flow rate and nozzle diameter were fixed at 308 K, 10 MPa, 1 mL/min and 100 μm, respectively. The results are shown in the experimental run numbers 1–4 in Table 2. The mean particle size of original sul-

fathiazole was  $43.0 \pm 15.5 \mu\text{m}$  observed from its SEM image. It is observed that smaller particles were obtained after the semicontinuous SAS treatment when acetone was used as the solvent, as indicated by comparing the results from run numbers 1 and 3 in Table 2. When the solution concentration was increased from 60 to 90% of its saturation value for each solvent, there were decreases in the mean particle size as shown in run numbers 2 and 4 in Table 2. The degree of supersaturation was higher at a higher solution concentration for each solvent. Therefore, the induction time for nucleation was shorter that caused the recrystallized smaller particles. Graphical comparison for the solvent and solution concentration effects in this study is shown in Fig. 2. It is demonstrated that the standard deviation (*SD*) of the particle size decreased

**Table 2**  
Results for sulfathiazole after SAS process under various operational conditions.

Exp. no.	Operational conditions						Particle size		Polymorph form
	<i>S</i>	<i>C</i> (% sat.)	<i>T</i> (K)	<i>P</i> (MPa)	<i>F</i> (mL/min)	<i>D<sub>n</sub></i> (μm)	Mean (μm)	<i>SD</i> (μm)	
Original	–	–	–	–	–	–	43.0	15.5	III
1	Acetone	60	308	10	1	100	4.9	2.1	I
2	Acetone	90	308	10	1	100	3.3	1.5	I
3	Ethanol	60	308	10	1	100	16.9	10.5	IV
4	Ethanol	90	308	10	1	100	12.7	6.4	IV
5	Acetone	90	308	12	1	100	2.2	1.1	I
6	Acetone	90	308	14	1	100	3.4	1.5	I
7	Acetone	90	318	10	1	100	3.8	1.6	I
8	Acetone	90	318	12	1	100	4.0	1.6	I
9	Acetone	90	318	14	1	100	3.5	1.5	I
10	Acetone	90	328	10	1	100	4.4	1.8	I
11	Acetone	90	328	12	1	100	5.9	2.1	I
12	Acetone	90	328	14	1	100	6.9	3.0	I
13	Acetone	90	308	12	1	200	2.3	1.2	I
14	Acetone	90	308	12	2	100	2.1	0.8	I
15	Acetone	90	308	12	2	200	2.1	1.1	I

The irregular crystal habit of the original and SAS processed sulfathiazole was observed from SEM images.

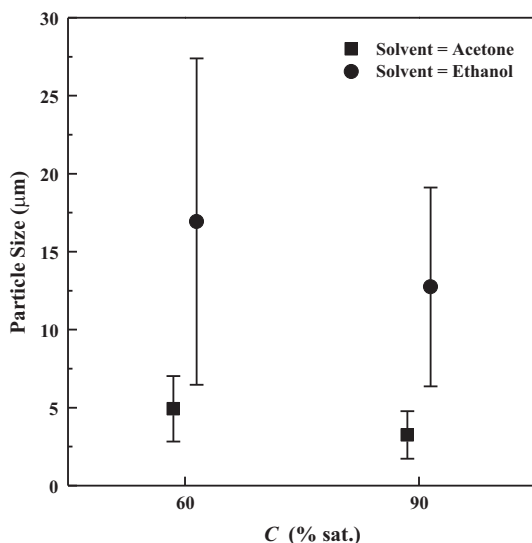


**Fig. 2.** Comparison of the particle size distribution for sulfathiazole due to solvent (S) and solution concentration (C) effects.

significantly after the SAS process. A more uniform particle size distribution was obtained after the SAS treatment.

The crystal structures for the original and SAS treated sulfathiazole in this study were examined using DSC and XRD. Five polymorphs of sulfathiazole have been reported in literature [13,14]. The DSC result of the original sulfathiazole is shown in Fig. 3(a) with two endothermic peaks at 449 K and 475 K. The first peak at a lower melting temperature was identical to that of polymorph form III [13,14]. In the DSC measurements, the original sulfathiazole first showed a solid–solid phase transition at 449 K from polymorph form III to form I. Upon continuously increasing the scanning temperature, we observed another solid–liquid tran-

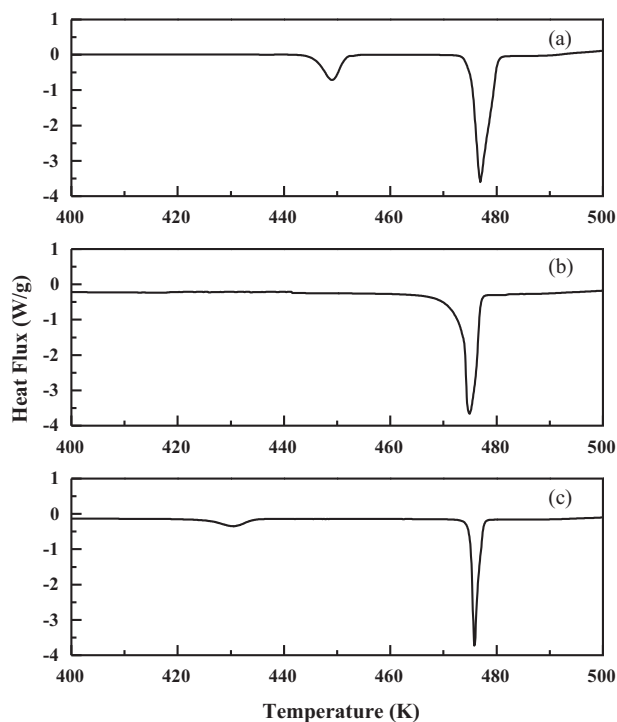


**Fig. 3.** DSC results of sulfathiazole: (a) original (polymorph form III); (b) SAS treated (Exp. run number 2 in Table 2, polymorph form I); (c) SAS treated (Exp. run number 4 in Table 2, polymorph form IV).

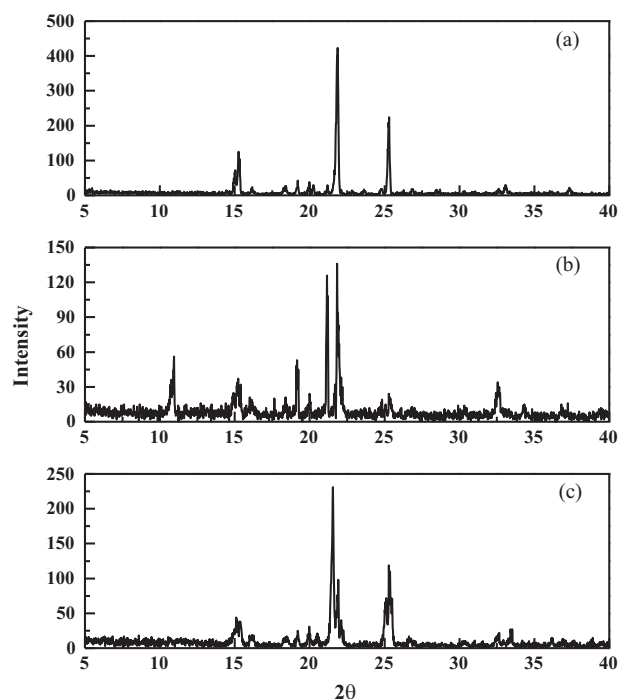


**Fig. 4.** XRD patterns for sulfathiazole: (a) original (polymorph form III); (b) SAS treated (Exp. run number 2 in Table 2, polymorph form I); (c) SAS treated (Exp. run number 4 in Table 2, polymorph form IV).

sition, or the melting of polymorph form I at 475 K. Fig. 3(b) shows that only one endothermic peak at 475 K was observed for polymorph form I, when acetone was used as the solvent in the SAS process. Fig. 3(c) demonstrates two endothermic peaks at 431 K and 475 K. The first peak showed a solid phase transition from polymorph form IV to form I, when ethanol was used as the solvent. The melting of polymorph form I was again observed at 475 K. The XRD patterns for the original and SAS treated sulfathiazole using two solvents are presented in Fig. 4. Through comparisons with the literature XRD patterns for various polymorphs of sulfathiazole, it is confirmed that the micronized particles with polymorph form I or form IV were obtained using acetone or ethanol as the solvent, respectively.

### 3.1.2. Effect of temperature and pressure

From the discussion in Section 3.1.1, acetone was selected as the solvent for the objective of smaller mean particle size after the SAS treatment. The solution concentration was maintained at a higher value of 90% saturation that was favorable to smaller particle production. We continued to investigate the temperature and pressure effects at the fixed solution flow rate of 1 mL/min and nozzle diameter of 100 µm. The results of temperature and pressure effects are shown in the experimental run numbers 2, and 5–12 in Table 2. At fixed operating pressure of 10 MPa, the mean particle sizes increased with temperature as shown by run numbers 2, 7 and 10 in Table 2. The possible explanation is owing to the decrease in degree of supersaturation at the higher operating temperature. The similar trend was observed at the fixed operating pressure of 12 MPa and 14 MPa, respectively.

The operation parameters in the antisolvent process often showed competing effects [18]. The process parameters of temperature and pressure had the competing effects in our SAS process. At a fixed temperature, increase of pressure might cause a higher volume expansion. This resulted in increasing nucleation rate and hence the smaller size particle formation. On the other hand, the increasing pressure might reduce the diffusion and evaporation

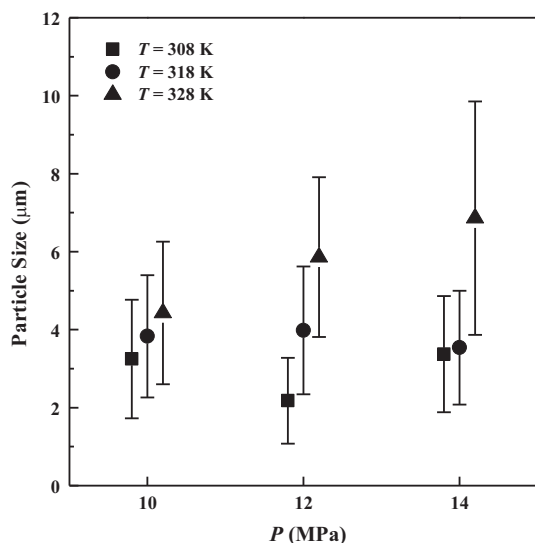


Fig. 5. Comparison of the particle size distribution for sulfathiazole due to temperature ( $T$ ) and pressure ( $P$ ) effects.

rate between  $\text{CO}_2$  and the organic solvent. This competing effect resulted in the aggregation of products and the larger size particle production. Temperature was another competing process parameter in our SAS experiments at a fixed pressure. The nucleation rate of sulfathiazole solute might increase with increasing temperature and resulted in smaller size particle production. The decrease in the degree of supersaturation with increasing temperature, however, caused larger size particle formation. Examining our experimental results shown in Table 2, the supersaturation effect was a dominant factor for the micronization of sulfathiazole.

At a fixed temperature of 308 K, the mean particle size firstly decreased with increasing pressure from 10 MPa to 12 MPa due to a higher volume expansion effect of  $\text{CO}_2$  as indicated by run numbers 2 and 5 in Table 2. The mean particle size increased again at an even higher pressure of 14 MPa as shown by run number 6 in Table 2. This is probably due to the aggregation of recrystallized sulfathiazole. At the operating temperature of 318 K, pressure effect on the resulting particle size was not obvious as shown by run numbers 7–9 in Table 2. This might be owing to the balance of the volume expansion and aggregation effects. The mean particle size increased with pressure at 328 K as shown by run numbers 10–12 in Table 2 where the aggregation of SAS treated products became more significant. Graphical comparison for all temperature and pressure effects in this study is illustrated in Fig. 5. The DSC and XRD examinations had been conducted for each experimental run. It is depicted in Table 2 that the original sulfathiazole changed from form III into form I when acetone was used as the solvent for all operating temperature and pressure conditions in our SAS experiments.

### 3.1.3. Effect of solution flow rate and nozzle diameter

From the discussions in Section 3.1.2, it is shown that the experimental condition at 308 K and 12 MPa yielded smaller mean particle size after the SAS treatment. We further investigated the effects due to solution flow rate and nozzle diameter at this operating temperature and pressure. The results are expressed by run numbers 13–15 in Table 2. The mixture critical points for the binary system of  $\text{CO}_2$  and acetone were 8.0 MPa and 9.6 MPa at 313 K and 333 K, respectively [19]. Our SAS operations were all in the homogeneous phase above the mixture critical points. The effects of nozzle diameter and solution flow rate were not significant owing to the similar improvement of mass transfer in our SAS processes.

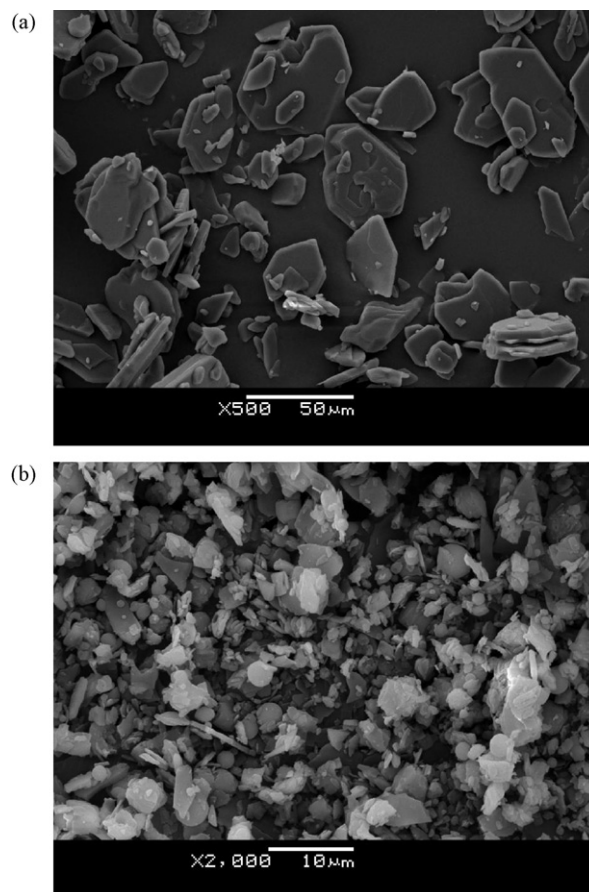


Fig. 6. SEM images for sulfathiazole: (a) original; (b) SAS treated (Exp. run number 14 in Table 2).

The optimal operating conditions were finally determined as experimental run number 14 in Table 2 with smaller mean particle size and its distribution. The mean particle size of sulfathiazole was micronized from its original value of  $43.0 \pm 15.5 \mu\text{m}$  to  $2.1 \pm 0.8 \mu\text{m}$ . Comparison of the SEM images of the original and micronized sulfathiazole particles at the optimal operating conditions is shown in Fig. 6. The crystal habits for the original and SAS processed sulfathiazole were all irregular as shown in Fig. 6(a) and (b), respectively. Graphical illustration for the particle size distribution (vol.%) between the original and SAS treated sulfathiazole at the optimal operating condition, measured by the dynamic laser scattering, is shown in Fig. 7. It is demonstrated that much smaller sulfathiazole particles with narrower size distribution were obtained after the semicontinuous SAS process.

### 3.2. Results for the dissolution rate of sulfathiazole

Three samples were investigated for the dissolution rate measurements: (1) the original sulfathiazole (polymorph form III), (2) the SAS treated sulfathiazole using acetone as the solvent (polymorph form I from experimental run number 14 in Table 2), and (3) the SAS treated sulfathiazole using ethanol as the solvent (polymorph form IV from experimental run number 4 in Table 2). The dissolution profiles are illustrated in Fig. 8. It is demonstrated that the SAS treated sulfathiazole yielded the higher dissolution rate. The dissolution rate of the micronized sulfathiazole with polymorph form I also showed more enhanced dissolution rate than that with polymorph form IV. In this study, two empirical models were applied to fit the dissolution rate data. The Weibull model [20]

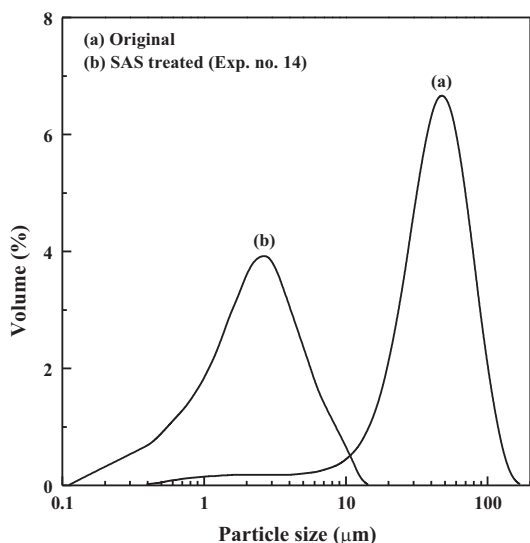


Fig. 7. Comparison of the particle size distributions for sulfathiazole before and after the SAS process.

was expressed as:

$$m = 1 - \exp\left(-\frac{t^b}{a}\right) \quad (1)$$

where  $m$  is the accumulated fraction of API in a dissolution medium at time  $t$ ,  $a$  and  $b$  are two empirical parameters that were optimally fitted using the experimental data. Based on the Weibull model, the dissolution rate coefficient ( $k_w$ ) was defined as the reciprocal of the time interval where 63.2% of the original amount of API has been dissolved. The dissolution rate coefficient ( $k_w$ ) has been adopted in literature for comparing the dissolution profiles [21,22]. It was calculated from the parameters in the Weibull model as:

$$k_w = \frac{1}{\sqrt[b]{a}} \quad (2)$$

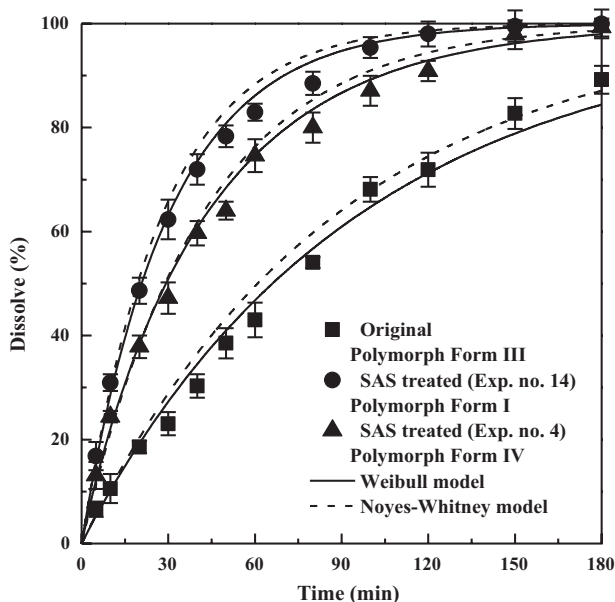


Fig. 8. Dissolution profiles for sulfathiazole in simulated intestinal fluid (pH=6.8) before and after the SAS processes.

Our experimental dissolution data were also fitted by the Noyes–Whitney model [23]:

$$m = 1 - \exp(-k_1 t) \quad (3)$$

where  $m$  is also the accumulated dissolved fraction of the API at time interval  $t$ , and  $k_1$  is a first order release constant. The  $k_1$  constant is related to the diffusion coefficient ( $D$ ) and the contacted surface area ( $S_a$ ) between the API and the dissolution medium as:

$$k_1 = \frac{DS_a}{Vh_d} \quad (4)$$

where  $V$  is the volume of the dissolution medium, and  $h_d$  is the thickness of the diffusion boundary layer.

The similarity for the behavior of dissolution profiles of a specific API is also important for pharmaceutical application. The difference factor ( $f_1$ ) and similarity factor ( $f_2$ ) were applied in this study to determine if the dissolution behavior of the SAS treated sulfathiazole was different from the original API. These two factors were defined as:

$$f_1 = \frac{\sum_{i=1}^n |R_i - T_i|}{\sum_{i=1}^n R_i} \times 100 \quad (5)$$

$$f_2 = 50 \times \log \left[ \left( 1 + \frac{1}{n} \sum_{i=1}^n |R_i - T_i|^2 \right)^{-0.5} \times 100 \right] \quad (6)$$

where  $R_i$  and  $T_i$  are the percentages of the dissolved sulfathiazole of the original and SAS treated samples at a time interval  $i$ , respectively. The summation in the above two equations are over all  $n$  data points. These factors have been used to compare the similarity of dissolution profiles for different dosage forms in literatures [24,25]. For different dissolution behaviors of two samples,  $f_1$  value should be greater than 15 and  $f_2$  value should be lower than 50. The similarity factor ( $f_2$ ) also has been adopted by food and drug administration (FDA) and European medicines agency (EMA) as a criterion for the assessment of dissolution profiles.

Table 3 lists the optimally fitted parameters of the Weibull and Noyes–Whitney models. The calculated dissolution rate constants of the Weibull model, the first order release constant of the Noyes–Whitney model, the difference factors, and the similarity factors are also shown in Table 3. The dissolution rate coefficient ( $k_w$ ) of the micronized sulfathiazole with polymorph form I and form IV showed higher dissolution rates by 3.2 and 2.2 times, respectively, than the original API with polymorph form III. The similar enhancement effect was obtained by examining the first order release constant ( $k_1$ ) of the Noyes–Whitney model. The difference factors ( $f_1$ ) for SAS treated and micronized sulfathiazole particles were greater than 15, and the similarity factors ( $f_2$ ) were also lower than 50. These results confirmed that the dissolution profiles after the SAS treatments were significantly different from the original sulfathiazole. It is also observed from Table 3 that the micronized sulfathiazole with polymorph form I had a greater degree of enhancement of dissolution when acetone was used as the solvent in the SAS process.

The enhanced dissolution rate of micronized particles is closely related to the increase in surface area [26]. The order of dissolution rates for various polymorphs of sulfathiazole measured in this study was consistent with those reported by Anwar and Khoshkhoo [27]. Polymorph I received in our SAS experiments had the lowest intensity of crystallinity shown by the XRD patterns in Fig. 4, and hence the highest dissolution rate. The interactions between the solvent and the recrystallized solid surface yielded the major contribution for the formation of polymorphs in the supercritical fluid process.

**Table 3**  
The calculated results for the dissolution of the original and SAS processed sulfathiazole.

API of sulfathiazole	Weibull model				Noyes–Whitney model		$f_1$	$f_2$
	$a$	$b$	$k_w$ ( $\text{min}^{-1}$ )	Degree of enhancement	$k_1$ ( $\text{min}^{-1}$ )	Degree of enhancement		
Original (polymorph form III)	89.19	0.984	0.0104	–	0.0114	–	–	–
SAS treated (Exp no. 14, polymorph form I)	28.50	0.985	0.0333	3.2	0.0358	3.2	62.8	26.0
SAS treated (Exp no. 4, polymorph form IV)	35.36	0.948	0.0233	2.2	0.0240	2.1	44.6	33.6

#### 4. Conclusion

The API of sulfathiazole was recrystallized and micronized in this study using the semicontinuous supercritical antisolvent process. The effects of the type of solvent, solution concentration, temperature, pressure, solution flow rate and nozzle diameter were experimentally investigated to obtain the smallest particles with the narrowest particle size distribution. The optimal operating conditions were determined when acetone was used as the solvent with solution concentration at 90% saturation. The optimal operating conditions were at 308 K, 12 MPa, solution flow rate of 2 mL/min (converted at the ambient condition) and nozzle diameter of 100  $\mu\text{m}$ . The resulting mean particle size at these optimal operating conditions was  $2.1 \pm 0.8 \mu\text{m}$  that was much smaller than the original mean size of  $43.0 \pm 15.5 \mu\text{m}$ . The micronized sulfathiazole at the optimal operating conditions had polymorphic form I. The dissolution rate of the optimally micronized sulfathiazole was enhanced to 3.2 times of the untreated particles.

#### Acknowledgement

The authors are grateful to the support of National Science Council, and Ministry of Economic Affairs, Taiwan, for supporting this research.

#### References

- [1] M. Bahrami, S. Ranjbarian, Production of micro- and nano-composite particles by supercritical carbon dioxide, *J. Supercrit. Fluids* 40 (2007) 263–283.
- [2] A. Martin, M.J. Cocero, Micronization processes with supercritical fluids: fundamentals and mechanisms, *Adv. Drug Deliv. Rev.* 60 (2008) 339–350.
- [3] T. Yasuji, H. Takeuchi, Y. Kawashima, Particle design of poorly water-soluble drug substances using supercritical fluid technologies, *Adv. Drug Deliv. Rev.* 60 (2008) 388–398.
- [4] J.O. Werling, P.G. Debenedetti, Numerical modeling of mass transfer in the supercritical antisolvent process, *J. Supercrit. Fluids* 16 (1999) 167–181.
- [5] J.O. Werling, P.G. Debenedetti, Numerical modeling of mass transfer in the supercritical antisolvent process: miscible conditions, *J. Supercrit. Fluids* 18 (2000) 11–24.
- [6] C.S. Lengsfeld, J.P. Delplanque, V.H. Barocas, T.W. Randolph, Mechanism governing microparticle morphology during precipitation by a compressed antisolvent: atomization vs nucleation and growth, *J. Phys. Chem. B* 104 (2000) 2725–2735.
- [7] F. Chavez, P.G. Debenedetti, J.J. Luo, R.N. Dave, R. Pfeffer, Estimation of the characteristic time scales in the supercritical antisolvent process, *Ind. Eng. Chem. Res.* 42 (2003) 3156–3162.
- [8] E. Reverchon, E. Torino, S. Dowy, A. Braeuer, A. Leipertz, Interactions of phase equilibria, jet fluid dynamics and mass transfer during supercritical antisolvent micronization, *Chem. Eng. J.* 156 (2010) 446–458.
- [9] Y.P. Chang, M. Tang, Y.P. Chen, Micronization of sulfamethoxazole using the supercritical anti-solvent process, *J. Mater. Sci.* 43 (2008) 2328–2335.
- [10] A. Kordikowski, M. Siddiqi, S. Palakodaty, Phase equilibria for the  $\text{CO}_2$  + methanol + sulfathiazole system at high pressure, *Fluid Phase Equilib.* 194–197 (2002) 905–917.
- [11] S.D. Yeo, M.S. Kim, J.C. Lee, Recrystallization of sulfathiazole and chlorpropamide using the supercritical antisolvent process, *J. Supercrit. Fluids* 25 (2003) 143–154.
- [12] G. Caputo, E. Reverchon, Use of urea as habit modifier in the supercritical antisolvent micronization of sulfathiazole, *Ind. Eng. Chem. Res.* 46 (2007) 4265–4272.
- [13] J. Anwar, S.E. Tarling, P. Barnes, Polymorphism of sulfathiazole, *J. Pharm. Sci.* 78 (1989) 337–342.
- [14] D.C. Apperley, R.A. Fletton, R.K. Harris, R.W. Lancaster, S. Tavener, T.L. Threlfall, Sulfathiazole polymorphism studied by magic-angle spinning NMR, *J. Pharm. Sci.* 88 (1999) 1275–1280.
- [15] E. Reverchon, R. Adami, G. Caputo, I. De Marco, Spherical microparticles production by supercritical antisolvent precipitation: interpretation of results, *J. Supercrit. Fluids* 47 (2008) 70–84.
- [16] M.D. Abramoff, P.J. Magelhaes, S.J. Ram, Image processing with ImageJ, *Biophotonics Inter.* 11 (2004) 36–42.
- [17] The United States Pharmacopodia, 32nd ed., United States Pharmacopodia Convention, Inc., Washington, DC, 2009.
- [18] F. Dehghani, N.R. Foster, Dense gas anti-solvent processes for pharmaceutical formulation, *Curr. Opin. Solid State Mater. Sci.* 7 (2003) 363–369.
- [19] T. Adrian, G. Maurer, Solubility of carbon dioxide in acetone and propionic acid at temperatures between 298 K and 333 K, *J. Chem. Eng. Data* 42 (1997) 668–672.
- [20] P. Costa, J. Manuel, S. Lobo, Modeling and comparison of dissolution profiles, *Eur. J. Pharm. Sci.* 13 (2001) 123–133.
- [21] H. Loth, E. Hemgesberg, Properties and dissolution of drugs micronized by crystallization from supercritical gases, *Int. J. Pharm.* 32 (1986) 265–267.
- [22] M. Charoenchaitrakool, F. Dehghani, N.R. Foster, H.K. Chan, Micronization by rapid expansion of supercritical solutions to enhance the dissolution rates of poorly water-soluble pharmaceuticals, *Ind. Eng. Chem. Res.* 39 (2000) 4794–4802.
- [23] A. Dokoumetzidis, V. Papadopoulou, P. Macheras, Analysis of dissolution data using modified versions of Noyes–Whitney equation and the Weibull function, *Pharm. Res.* 23 (2006) 256–261.
- [24] V. Pillay, R. Fassihi, Evaluation and comparison of dissolution data derived from different modified release dosage forms: an alternative method, *J. Control. Release* 55 (1998) 45–55.
- [25] J.E. Polli, G.S. Rekhi, L.L. Augsburger, V.P. Shah, Methods to compare dissolution profiles and a rationale for wide dissolution specifications for metoprolol tartrate tablets, *J. Pharm. Sci.* 86 (1997) 690–700.
- [26] M. Mosharraf, C. Nystrom, The effect of particle size and shape on the surface specific dissolution rate of microsized practically insoluble drugs, *Int. J. Pharm.* 122 (1995) 35–47.
- [27] J. Anwar, S. Khoshkhoo, Crystallization of polymorphs: the effect of solvent, *J. Phys. D: Appl. Phys.* 26 (1993) B90–B93.